Computational Studies of Iodinated Coumarin Derivative by Density Functional Theory

Manjula Katageri, Sulochana Devar**, Vijayalaxmi Mallayya*** & S.M. Hanagodimath*****

DOI: https://doi.org/10.5281/zenodo.21223719

ABSTRACT

The photophysical properties of the iodinated coumarin derivative 4-(3-Iodo-phenoxymethyl)-6-methyl-chromen-2-one [4(3IP)6MC] has been studied using computational methods, using Gaussian 16W software in Density functional theory (DFT) with the B3LYP/3-21G level. The physical and chemical properties of 4(3IP)6MC have been studied. We have estimated the dipole moment, to identify the molecular stability frontier molecular orbitals (FMO), and the molecular electrostatic potential (MEP) investigates the coumarin molecule preferred locations for electrophilic and nucleophilic attacks. The distribution of Mulliken atomic charges has been performed. The nonlinear optical properties (NLO) have been calculated: dipole moment, polarizability, and first-order hyperpolarizabilities. The intermolecular interactions identified with natural bonding orbital (NBO) have been studied, and the temperature dependency of the thermodynamic characteristics has been analyzed. This iodinated coumarin derivative has advanced optical and imaging applications.

KEYWORDS: *Density Function Theory (DFT), Dipole Moment, Frontier Molecular Orbitals (FMO), Molecular Electrostatic Potential (MEP), Nonlinear Optical Properties (NLO).*

Introduction

Heterocyclic oxygen-containing coumarin derivatives are widely found in numerous natural products. They exhibit a broad spectrum of biological activities, including antibacterial, antimalarial, anticancer, anti-HIV, analgesic, antioxidant, and anti-inflammatory effects [1–2]. In recent decades, cancer has emerged as one of the leading causes of mortality worldwide and remains a complex, life-threatening disease affecting multiple organs of the human body. Coumarin derivatives readily interact with various enzymes and biological receptors, which makes them promising candidates for therapeutic applications. Their structural versatility allows them to serve as potential pharmacologically active agents.

In contemporary research, considerable attention has been directed toward investigating the photophysical properties of newly synthesized iodinated coumarin derivatives. The incorporation of iodine into the molecular framework is particularly significant due to its distinctive photophysical characteristics, such as high polarizability and its ability to participate in specific molecular interactions. Iodine substitution can influence biological activity and has been reported to modulate interactions with targets such as cannabinoid receptors, thereby affecting diverse biological pathways [3-4]. In the present study, a iodinated 4-aryloxymethyl coumarin derivative, 4-(3-Iodo-phenoxymethyl)-6-methyl-chromen-2-one [4(3IP)6MC], was synthesized [5]. The theoretical computational photophysical properties was investigated using Gaussian 16W software, employing the DFT/B3LYP in the 3-21G base set. The dipole moment, Mulliken atomic charges, Fortier molecular orbital (HOMO-LUMO) energies, the molecular electrostatic potential map (MEP), natural bond orbital (NBO), nonlinear optical (NLO), and thermodynamic properties of the molecule 4(3IP)6MC were calculated and

* **Dr. Manjula Katageri,** Associate Professor, Government First Grade Residential SC/ST's Model College, Hadalageri, Muddebihal.

** **Sulochana Devar,** Guest Lecturer, Department of PG Studies and Research in Physics, Gulbarga University, Kalaburagi.

*** **Vijayalaxmi Mallayya,** Guest Lecturer, Government Autonomous College, Kalaburagi.

**** **Dr. S.M. Hanagodimath,** Senior Professor and Research Supervisor, Department of PG Studies and Research in Physics, Gulbarga University, Kalaburagi.

analyzed with the optimized geometry using density functional theory.

Materials and Methods

The iodine-based coumarin derivative, 4-(3-Iodo-phenoxymethyl)-6-methyl-chromen-2-one [4(3IP)6MC], was synthesized by following the method outlined in reference [5]. Its molecular structure is presented in Fig. 1. For theoretical computational study, Gaussian 16W software supports simulations ranging from small molecules to complex macromolecules with different methods such as Hartree-Fock (HF), semi-empirical, and Density functional theory (DFT). Among all methods, the DFT/B3LYP method with a 3-21G basis set, particularly the most efficient for the geometry of the iodinated coumarin derivative molecule, was used. In the gas phase, the optimization was carried out. The improved geometry has been utilized for the subsequent computations [6-10].

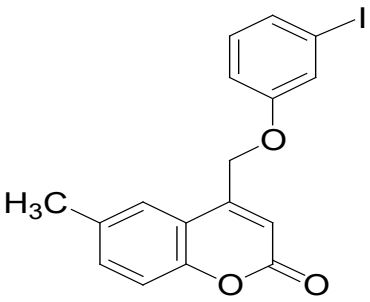

Fig. 1: Structure of 4(3IP)6MC

Results and Discussion

3.1 Optimized Structure of 4(3IP)6MC

The molecular geometry of 4(3IP)6MC was optimized using the Gaussian 16W software, employing the DFT/B3LYP in the 3-21G base set [10]. The optimized structure, along with the vector of the dipole moment, is illustrated in Fig. 2. The computational ground-state dipole moment is found to be 6.47 D for 4(3IP)6MC.

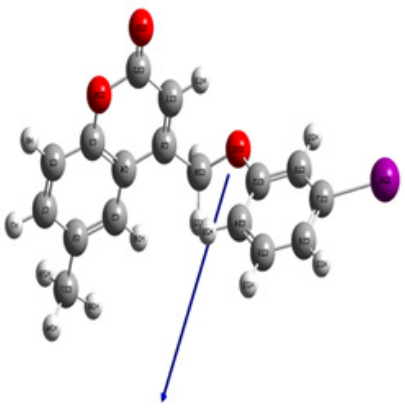

Fig. 2: Optimized structure with dipole moment vector of 4(3IP)6MC

3.2 Frontier Molecular Orbital (FMO)

Frontier molecular orbital energies were employed to assess the reactivity, stability, and interaction characteristics of the compounds. These are HOMO, the highest occupied molecular orbital, which acts as an electron donor and has a strong nucleophile and LUMO, the lowest unoccupied molecular orbital, which acts as an electron acceptor and has a pronounced electrophilic character. The behavior of a pair of electrons within a molecule is described through HOMO and LUMO energies with ionization potential (Z) and electron affinity (E). The parameters of global reactivity descriptors such as electronegativity (=(Z+E)/2), chemical potential (μ=-(Z+E)/2), chemical hardness (= (Z-E)/2), chemical softness (= 1/2), and electrophilicity index (= μ2/2). The energy band gap between HOMO and LUMO orbitals serves as molecular stability. The larger the band gap, the greater the stability and the lower the chemical reactivity, whereas a smaller gap enhances reactivity and facilitates electron transfer. The frontier molecular orbital (FMO) surfaces of HOMO and LUMO are depicted in Fig. 3 for 4(3IP)6MC computed in the vacuum phase. Based on HOMO-LUMO energy, the ionization potential and electron affinity are (-0.2338 eV) and (-0.0741 eV). The chemical softness (6.2617 eV), electronegativity (0.1539), and chemical potential (-0.1539) reveal a more uneven electron density distribution and a greater tendency for electrons to escape from the equilibrium system. The electrophilicity (0.1484) index further clarifies that the electron-accepting capability exhibits stronger ICT characteristics, and the molecule is more stabilized in an excited state. The FMO parameters of molecule in vacuum phase are given in Table 1[11-13].

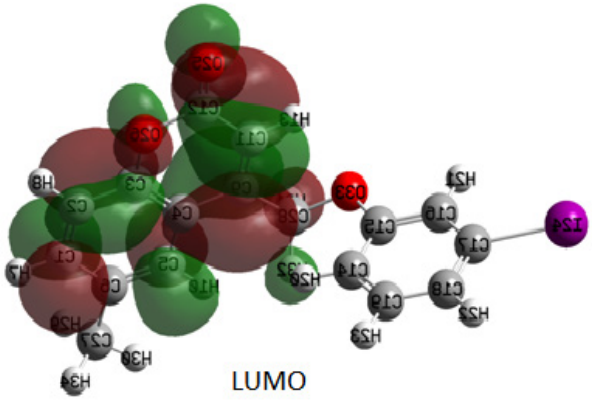

Calculated Values:

ELUMO = -0.0741 eV

ΔE = -0.1597 eV

EHOMO = -0.2338 eV

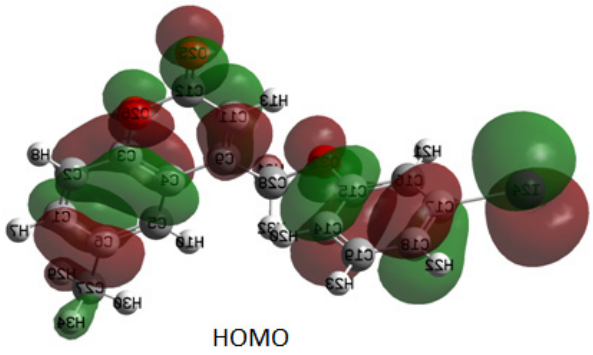

Fig. 3: HOMO and LUMO surfaces of 4(3IP)6MC

Table 1. Calculated energy values of global reactivity descriptors of 4(3IP)6MC

Coumarin molecule	4(3IP)6MC
EHOMO in eV	-0.2338
ELUMO in eV	-0.0741
Δ E-Energy gap in eV	0.1597
Z-Ionization potential in eV	0.2338
E-Electron affinity in eV	0.0741
χ -Electro negativity in eV	0.1539
μ- Chemical potential in eV	-0.1539
Ƞ- Chemical hardness in eV	0.0798
σ-Chemical softness in eV-1	6.2617
ω-Electrophilicity in eV	0.1484

3.3 Molecular Electrostatic Potential (MEP)

The molecular electrostatic potential (MEP) maps and their contours of 4(3IP)6MC were visualized in Figs. 4(a) and (b). The distribution of charges is depicted with various colors. The strong blue nucleophile region on the donor indicates the most positive electrostatic potential, which is prone to electrophilic attack. The strong red electrophilic region of acceptor shows the most negative electrostatic potential, favouring nucleophilic attack. The electrostatic potential for 4(3IP)6MC falls between −6.455 a.u. (dark red) and +6.455 a.u. (dark blue) . The oxygen atom bound to the carbon atom is the primary location of the negative electrostatic potential, indicating that this site is most vulnerable to electrophilic assault. On the other hand, the hydrogen (H) and iodine (I) atoms bonded to the benzene ring exhibit positive electrostatic potential, which is advantageous for nucleophilic attack. The order of increasing potential values is red < orange < yellow < green < blue. Colors are used to depict the change in electrostatic potential. Strong potential gradients and high polarity are indicated by closely spaced contours in an MEP contour map, while low polarity and less reactive areas are indicated by widely spread contours.

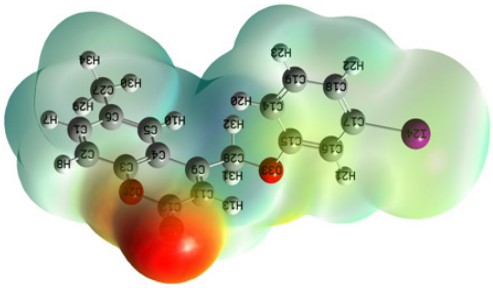

Fig. 4 (a) MEP map of 4(3IP)6MC

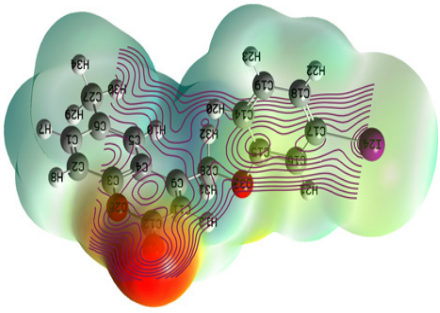

(b) MEP Contour map of 4(3IP)6MC)

3.4 Mulliken Atomic Charges

Mulliken population analysis reveals pronounced charge distribution within the molecular framework of 4(3IP)6MC. Using DFT/B3LYP/3-21G level in the gas phase, the value of atomic charges are studied and are given in Table 2. From optimized geometry, from charges of atoms, the chemical composition of the molecule is predicted. In atomic charge distribution, the molecule consists of iodine, carbon, hydrogen, and oxygen atoms. Hydrogen atoms are positive due to electron sharing with neighbouring atoms. The oxygen atoms O25, O26, and O33 exhibit substantial negative charges (–0.472 to –0.527), indicating strong electron-donating capability. Notably, C27 carries a remarkably high negative charge (–0.779), reflecting significant resonance-assisted electron accumulation. In contrast, the carbonyl carbon (C12) shows a large positive charge (+0.614), confirming its strong electron-accepting nature. The iodine substituent also displays positive polarization (+0.291), suggesting an inductive electron-withdrawing effect. This distinct donor–π–acceptor arrangement promotes intramolecular charge transfer across the conjugated backbone. The data is visually shown in Fig. 5, offering a clear view of charge distribution patterns across solvents [13].

Table 2. Mulliken atomic charges of 4(3IP)6MC

Atom	Gas Phase	Atom	Gas Phase
1 C	-0.1764	18 C	-0.1533
2 C	-0.1709	19 C	-0.1852
3 C	0.2337	20 H	0.2457
4 C	0.0280	21 H	0.2324
5 C	-0.2407	22 H	0.2161
6 C	-0.0855	23 H	0.2127
7 H	0.2035	24 I	0.2918
8 H	0.2238	25 O	-0.4724
9 C	-0.0828	26 O	-0.5272
10 H	0.1774	27 C	-0.7794
11 C	-0.2690	28 C	-0.3240
12 C	0.6146	29 H	0.2953
13 H	0.2514	30 H	0.3032
14 C	-0.2134	31 H	0.3329
15 C	0.2392	32 H	0.3205
16 C	-0.1770	33 O	-0.4961
17 C	-0.3997	34 H	0.3306

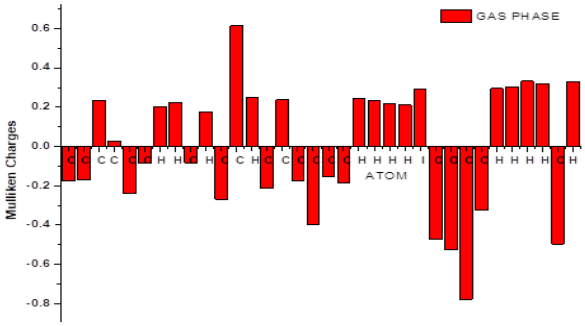

Fig. 5: Mulliken atomic Charge distribution of 4(3IP)6MC

3.5 Natural Bond Orbital (NBO)

For intra- and intermolecular bond interactions in molecular systems, NBO analysis is an essential tool. To evaluate the donor and acceptor relationships in the NBO study, a second-order Fock matrix was used. This represents perturbation energy used to find bonding and antibonding interactions caused by second-order disturbance. For every donor (i) and acceptor (j), the stabilization energy E(2) related to delocalization terms i and j is given by Eq.(1).

$$E(2) = \Delta E_{ij} = q_i \frac{(F_{ij})^2}{(E_j - E_i)}$$

where qi represents the donor orbital population. Ei and Ej are the diagonal elements, and Fij represents the off-diagonal Fock matrix element of NBOs. In stabilization energy E(2), there are σ and π, two types of acceptors and donors, respectively. The higher the second-order stabilization energy E(2) value, the more interaction between electron donors and acceptors and the larger the amount of conjugation of the complete structure. Employing the DFT/B3LYP in the 3-21G base set to compute the NBO calculations.

The NBO second-order perturbation analysis reveals pronounced π → π* interactions within the conjugated framework of the molecule 4(3IP)6MC. The most significant interactions of coumarin derivative among all interactions are represented in Table 3. The most significant stabilization energies are observed for π(C9–C11) → π*(C12–O25) (23.44 kcal/mol), π(C1–C2) →

Table 3. Second order perturbation analyses of Fock matrix in NBO basis of 4(3IP)6MC

Donor (i)	Occupancy	Acceptor(j)	Occupancy	E2(j) (Kj/mol)a	E(j)-E(i) (a.u)b	F(ij) (a.u)c
π(C1-C2)	1.701	π*C3-C4)	0.446	21.36	0.26	0.070
π(C1-C2)	1.701	π* (C5-C6)	0.313	18.43	0.28	0.065
π(C3-C4)	1.611	π* (C5-C6)	0.313	18.19	0.29	0.063
σ ((C9-C11)	1.975	σ*(C4-C9)	0.031	4.33	1.25	0.066
π(C9-C11)	1.819	π* (C12-O25)	0.015	23.44	0.28	0.075
π(C12-O25)	1.996	π* (C12-O25)	0.295	1.06	0.36	0.019
σ ((C14-C15)	1.980	σ*((C15-C16)	0.026	4.46	1.29	0.068
π(C14-C15)	1.667	π* (C18-C19)	0.330	21.15	0.29	0.070
π(C15-C16)	1.968	π* (C17-I24)	0.031	3.99	0.75	0.049
π (C16-C17)	1.712	π* (C14-C15)	0.400	19.60	0.28	0.068
π (C18-C19)	1.971	π* (C17-I24)	0.031	4.28	0.73	0.050
π(C18-C19)	1.679	π* (C14-C15)	0.400	18.52	0.26	0.064
π(C18-C19)	1.679	π*C16-C17)	0.371	21.69	0.26	0.068

π*(C3–C4) (21.36 kcal/mol), and π(C18–C19) → π*(C16–C17) (21.69 kcal/mol), indicating strong electron delocalization across the aromatic and carbonyl moieties. These high stabilization energies confirm the presence of extended conjugation and efficient intramolecular charge transfer (ICT) from the electron-rich aromatic system toward the electron-deficient carbonyl group. The interaction involving the carbonyl π*(C=O) orbital demonstrates its crucial role as an electron acceptor, stabilizing the excited state and contributing to the bathochromic shift observed experimentally. Moderate interactions involving the C–I bond suggest minor halogen-assisted delocalization effects. These NBO results strongly support the extended π-conjugation and charge transfer character responsible for the photophysical behavior of the molecule [14].

3.6 Non-linear Optical (NLO) Properties

The materials respond nonlinearly to the charge distribution polarization induced by the interaction of a substance with electromagnetic radiation. The non-linear properties have a vital role in the area of optical modulation in telecommunication, dynamic image processing, signal processing, and optical interconnections. The responsibility for NLO features is the delocalization of electrons in organic molecules, which increases polarizability and causes their mean initial hyperpolarization to increase. The NLO properties response of an isolated molecule subjected to an external electric field is characterized by its electric dipole moment (μ), polarizability (α), and first- and second-order hyperpolarizabilities (β and γ) [14-15]. The Taylor series expansion provides the total dipole moment (μ_{tot}), the static polarizability (α_0), the anisotropy of polarizabilities ($\Delta\alpha$), and the static hyperpolarizability of first-order (β_0), which are extracted and presented in Eqs. (2) to (5). The correlations between molecular structure, dipole moment, polarizability, and first-order hyperpolarizability of 4(3IP)6MC.

$$\mu = \sqrt{\mu_x^2 + \mu_y^2 + \mu_z^2}, \quad (2)$$

$$\alpha_o = \frac{[\alpha_{xx} + \alpha_{yy} + \alpha_{zz}]}{3} \quad (3)$$

$$\Delta\alpha = \sqrt{\frac{[\alpha_{xx} - \alpha_{yy}]^2 + [\alpha_{yy} - \alpha_{zz}]^2 + [\alpha_{zz} - \alpha_{xx}]^2 + 6\alpha_{xz}^2}{2}} \quad (4)$$

$$\beta_o = \sqrt{[\beta_{xxx} + \beta_{xyy} + \beta_{xzz}]^2 + [\beta_{yyy} + \beta_{yxx} + \beta_{yzz}]^2 + [\beta_{zzz} + \beta_{zxx} + \beta_{zyy}]^2} \quad (5)$$

The nonlinear optical (NLO) parameters of 4(3IP)6MC were computed using the optimized geometry obtained at the DFT/B3LYP/3-21G base set, and results are summarized in Table 4. The key results include a dipole moment (μtot) of 6.471D for 4(3IP)6MC, which exceeds the value of the standard NLO reference urea (3.9 D). The molecular polarizability (α0) for 4(3IP)6MC is 29.317 × 10^{-}24 esu, whereas for urea: 3.749 × 10^{-}24esu. The first-order hyperpolarizability (β0) for 4(3IP)6MC is 1.84 × 10^{-}30esu, and urea has 0.3728 × 10^{-}30esu. A comparative analysis with urea, the molecule exhibits significantly enhanced NLO responses. Polarizability and hyperpolarizability values of 4(3IP)6MC indicate a strong response to external electric fields, highlighting its potential as an efficient nonlinear optical material for advanced imaging applications [16-19].

Table 4. NLO properties of 4(3IP)6MC

μ	Electric Dipole Moment (Debye)	α	Polarizabilty (10-24) esu	β	First order hyper polarizabilty (10-30) esu
μx	-5.667	αxx	28.207	βxxx	-0.521
μy	-1.245	αxy	10.166	βyxx	0.420
μz	-2.864	αyy	39.108	βxyy	-0.251
μtot	6.471	αxz	40.716	βyyy	0.216
		αyz	0.681	βzxx	-0.145
		αzz	20.637	βxyz	-0.158
		α0	29.317	βzyy	1.562
		Δ α	72.330	βxzz	-0.469
				βyzz	0.125
				βzzz	-0.292
				β	1.84

3.7 Thermodynamic Properties

The temperature-dependent thermodynamic parameters reveal a continuous increase in heat capacity, entropy, and thermal energy with rising temperature [17-19]. The results are tabulated in Table 5. The rapid increase in heat capacity at lower temperatures is attributed to the progressive activation of vibrational modes. The monotonic rise in entropy indicates enhanced molecular flexibility and an increased population of vibrational states at elevated temperatures. The nature of thermodynamic properties is shown in Fig. 6. It shows the thermal energy and entropy of the 4(3IP)6MC molecule are the same at the temperature of 375K. These results suggest that at higher temperatures, non-radioactive decay pathways become more favorable, which may contribute to fluorescence quenching in the studied molecule.

Table 5. Thermodynamic properties of 4(3IP)6MC by DFT/B3LYP/3-21G method.

T(K)	CV (Cal mol-1k-1)	S (Cal mol-1k-1)	E-Thermal (Kcal mol-1)
100	31.04	99.36	153.10
200	50.81	128.29	157.18
300	71.58	153.61	163.30
400	91.36	177.54	171.46
500	108.22	200.24	181.47
600	121.98	221.59	193.06
700	133.15	241.57	205.78
800	142.27	260.23	219.56
900	149.75	277.67	234.18
1000	155.93	293.99	249.47

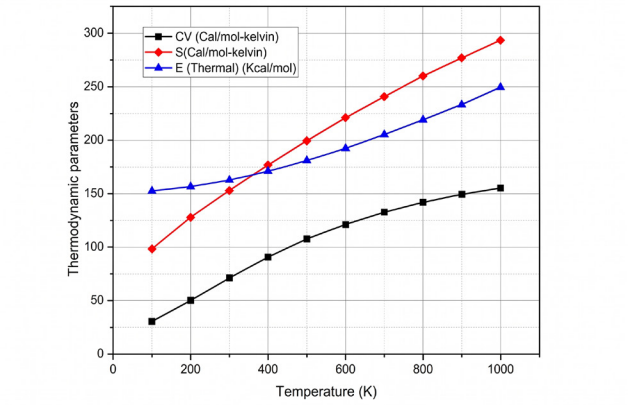

Fig. 6: Thermodynamic Properties of 4(3IP)6MC

Conclusions

In the present work, the photophysical properties of 4(3IP)6MC were studied using a quantum computational study with the DFT/B3LYP/3-21G method of Gaussian 16. In FMO, the HOMO-LUMO molecular chemical potential, hardness, softness, and electrophilicity were calculated. The reduced energy gap supports stronger ICT characteristics, and the molecule is more stabilized in an excited state. Mulliken atomic charge analysis shows pronounced charge polarization within the molecular framework. In MEP, the oxygen atom bound to the carbon is most vulnerable to electrophilic assault. The hydrogen (H) and iodine (I) atoms bonded to the benzene ring in nucleophilic attack. The NBO results strongly support the extended π-conjugation. The molecule exhibits significantly enhanced polarizability and hyperpolarizability responses of NLO. The temperature-dependent thermodynamic parameters reveal a continuous increase in heat capacity, entropy, and thermal energy with rising temperature. This analyzed and computed data for iodinated coumarin derivative has advanced optical and imaging medical applications.

Acknowledgment: The authors are thankful to the Photophysical lab for providing the Gaussian Windows 16W software for theoretical calculation at the Department of Physics, Gulbarga University, Kalaburagi.

Author Contribution: All authors contributed significantly to this research work. Manjula Katageri, Sulochana Devar, and Vijayalaxmi M. prepared the materials and collected and analyzed the data. The initial draft of the manuscript was prepared by Manjula Katageri, and all co-authors reviewed and approved the final version of the manuscript. The work was supervised by Professor S. M. Hanagodimath.

Data Availability: During the current investigation, no data sets were created; the manuscript had only occurred data.

Declarations: The authors declare that no funds, grants, or other support were received during the preparation of this manuscript.

Competing Interests: The authors declare no competing interests.

References:

1. Mohd A, Shahnaaz K et. Al. (2025) Exploring the anticancer potential and mechanisms of action of natural coumarins and isocoumarins, Europiean Journal of medical chemistry Vol.282.15 January,117088, https://doi.org/10.1016/j.ejmech.2024.117088.
2. Ljiungman M. (2009) Targeting the DNA danger response in cancer. Chem Rev.109,2929-2950, DOI: 10.1021/cr900047g.
3. M. A. Musa, J. S. Cooperwood, and M. O. Khan, (2008) A review of coumarin derivatives in pharmacotherapy of breast cancer, Curr. Med. Chem., vol. 15, pp. 2664–2679.
4. M. Curini, G. Cravotto, F. Epifano, and G. Giannone, (2006) Chemistry and biological activity of natural and synthetic phenyloxy coumarins, Curr. Med. Chem., vol. 13, pp. 199–222.
5. Mahantesha B, Vishwanath B. Jambagi, Nivedita N. Barigidad, Sandeep S. Laxmeshwar, Venkatesh D, Narayanachar (2014) Synthesis, structure activity relationship of iodinated-4- aryloxymethyl-coumarins as potential anti-cancer and antimycobacterial agents European Journal of Medicinal Chemistry 74, 225, e233. http://www.elsevier.com/locate/ejmech
6. Srinath, D. Lalasangi, V.Mallayya, S. M. Hanagodimath,(2025) Fluorescence Quenching Analysis of 6MNPM Molecule by Steady State Method||. g analysis of 6MNPM molecule Mapana – Journal of Sciences, Vol. 24, No. 1, 43-52 ISSN 0975-3303. https://doi.org/10.12723/mjs.72.3
7. Manjula katageri, Srinath, Shivaleela B, Sulochana Devar, S.M.Hanagodimath, (2025) Iodinated 4(3IP)BC Coumarin Derivative Dipole Moments by a Solvatochromic Shift Method and DFT Approach. Mapana Journal of Science, Vol.24, No.4, 1-21, https://doi.org/10.12723/mjs.75.1
8. Sulochana Devar, Srinath More, Omnath Patil, Basavaraj S.M.Nagesh G.Y, S.M. Hanagodimath,(2025) Synthesis, Spectroscopic, DFT Calculation and Molecular docking studies of Indole derivative, Journal of Fluorescence , 14, Springer, 10.1007/s10895-025-04301-2.
9. Sulochana Devar, Srinath More, Omnath Patil, Basavaraj S. M.Nagesh G.Y, S.M. Hanagodimath, (2023) Quantum Chemical Calculation And Molecular Docking Studies Of Indole Derivative, Section A-Research Paper Eur. Chem. Bull. 2023, 12(Special Issue 5), 6704 – 6717, DOI: 10.48047/ecb/2023.12.si5a.0603
10. M.A.Robb, (2022) "New Chemistry with Gaussian 16 and Gauss view 6" Jan1916, Accessed Sep, 25.
11. Shivaleela B, Shivaraj G, Ohmnath P, Hanagodimath S. M (2021). Quenching of fluorescence, Dipole moments and DFT Studied of newly synthasized Amino-Thiadiazole Coumarin derivative" J.of M.Shivajirao University, Baroda ISSN: 0025-0422., Vol.55(1),PP 200-218.
12. L. Fomekong Tsague, G.W. Ejuh, A. Teyou Ngoupo, Y. Tadjouteu Assatse, R.A. Yossa Kamsi, M.T. Ottou Abe, J.M.B. Ndjaka,(2023) Ab-initio and density functional theory (DFT) computational study of the effect of fluorine on the electronic, optical, thermodynamic, hole and electron transport properties of the circumanthracene molecule, Heliyo ttps://doi.org/10.1016/j.heliyon.2023.e19647
13. Shivaraj G. Gonnalli, Shivaleela B. Basavaraj, S.M.Hanagodimath, (2021) Spectroscopic analysis of NMR, IR, UV-VIS, HOMO-LUMO ESP and Mulliken charges of Coumarin derivatives by density Functional theory."Journal of the maharaja Sayajirao University of Baroda ISSN: 0025-0422, 55(1), 213-229.
14. B. Shivaleela, G.G.Shivaraj, S.M.Hanagodimath,(2023) Estimation of dipole moments by solvatochromic shift method, spectroscopic analysis of UV-Visible, HOMO-LUMO, ESP map, Mulliken atomic charges, NBO,NLO properties of Benzofuran derivative, Results in chemistry 6,101046. https://doi.org/10.1016/j.rechem.2023.101046
15. Chandrasekhar, S.; Deepa, H. R.; Melavanki, R. M.; Mogurampelly, S.; Basanagouda, M. M.; Yallappa, S.; Thipperudrappa, J. (2020) Quantum chemical and solvatochromic studies of biologically active 1,3,4-thiadiazol coumarin derivatives, Chemical Data Collections 29, 100516. https://doi.org/10.1016/j.cdc.2020.100516
16. Gonnalli S G, Basavaraj S, Hanagodimath S M (2021) Spectroscopic analysis of NMR, IR, UV–Vis, HOMO–LUMO, ESP and Mulliken charges of coumarin derivatives by density functional theory. Journal of the Maharaja Sayajirao University of Baroda. ISSN 0025-0422. Vol. 55, No. 1 (XIV), pp. 213–229.
17. Srinath. Ohmnath P, Sulochana D, and S.M.Hanagodimath (2024) Estimation of electric dipole moment by solvatochromism, computational method, and study of the effect of solvents by preferential solvation of 6-methoxy-4-(4-nitro-phenoxy methyl)-chromen-2-one (6MNPM), Journal of .Fluorescence. DOI: 10.1007/s10895-024-03955-8
18. Jayarajan R, Satheeshkumar R, Kottha T, Subbaramanian S, Sayin K, Vasuki G (2020) Water mediated synthesis of 6-amino-5-cyano-2-oxo-N-(pyridin-2-yl)-4-(p-tolyl)-2H-[1,2′-bipyridine]-3-carboxamide and 6-amino-5-cyano-4-(4-fluorophenyl)-2-oxo-N-(pyridin-2-yl)-2H-[1,2′-bipyridine]-3-carboxamide–An experimental and computational studies with nonlinear optical (NLO) and molecular docking analyses. Spectro chimica Acta PartA: Molecular and Bimolecular Spectroscopy 229:117861. https://doi.org/10.1016/j.saa.2019.117861.
19. Choudhary V K, Bhatt A K, Dash D, Sharma N (2019) DFT calculations on molecular structure, HOMO–LUMO study, reactivity descriptions and spectral analysis of newly synthesized diorganotin(IV) 2-chloridophenylacetohydroxamate complexes. Journal of Computational Chemistry 40(27):2354–2363. https://doi.org/10.1002/jcc.26012